

Microhardness and Microstructure on Welding of Nodular Cast Iron Grade FCD 500

Petchsang S.

Graduate Student, Production Engineering Department, Faculty of Engineering, KMUTT, Bangkok, Thailand

Poopat B.

Production Engineering Department, Faculty of Engineering, KMUTT, Bangkok, Thailand

Phung-on I.

MTC, Institute for Scientific and Technology Research and Services (ISTRs), KMUTT, Bangkok, Thailand

Abstract

The aim of this research is to study the microhardness and the microstructure of the welds of nodular cast iron by SMAW process utilizing two different patterns of filler metal: one uses only ENiFe-CI and the other employs ENiFe-CI as butter layer and followed by E7016. These investigations represent that the highest hardness occurs in the fusion boundary due to carbide formation; the HAZ composes of the formation of bainite and the bottom of the E7016 weld metal comprises martensite. On the contrary, the base metal and the ENiFe-CI weld metal gives lower hardness because of the formation of pearlite and graphite nodules surrounded by ferrite rings and austenite with ferrite at the sub-grain boundary respectively.

Keywords: *Nodular Cast Iron, Fusion Boundary, Heat Affected Zone*

1 Introduction

Nodular cast iron acquires from developing grey cast iron by adding magnesium before casting. This special technique can produce irons with the graphite spheroids instead of the graphite flakes. The compact shape of graphite improves the mechanical properties resulting in high strength and ductility toughness than those of grey cast iron [1].

Nevertheless, nodular cast iron has poor weldability owing to the formation of hard brittle phases, namely martensite and iron carbide at the weld interface [2,3]. This causes low elongation properties and high hardness values [2].

The objective of this research is to study the microhardness distribution in the different areas of the welds and the correlation with their microstructures resulted from shield metal arc welding (SMAW) process. The samples employ two different patterns of filler metal: one uses ENiFe-CI electrode because of having low coefficient of expansion and for the other, the first layer was applied ENiFe-CI electrode as the butter layer followed by E7016 electrode as the second layer and

built-up to the surface of the welding specimen in which it could provide higher strength compared to all ENiFe-CI electrode which has lower strength.

2 Theory

2.1 Nodular Cast Iron

This specific cast iron is referred to as a nodular cast iron, spheroidal graphite cast iron, or ductile cast iron owing to the spheroid form graphite. Nodular cast iron attains from improving grey cast iron that contains 3.2-4.5% of carbon and 1.8-2.8% of silicon with magnesium or cerium additions prior to casting. In addition, nodular cast iron constitutes lower sulfur (e.g., 0.08% max) and phosphorus (e.g., 0.02 % max) than gray cast iron in order to encourage the formation of spheroid graphite [1]. The matrix of nodular cast iron is generally pearlite, ferrite or their mixture [4], as shown in Figure 1.

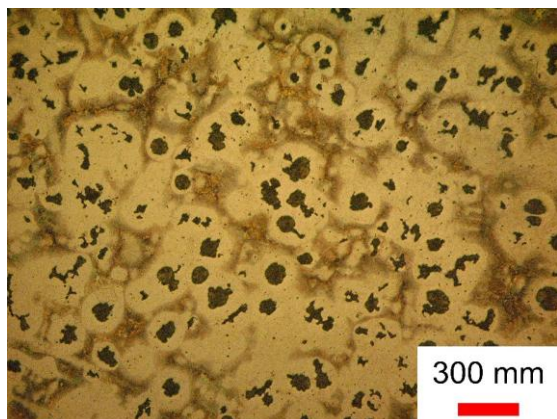


Figure 1: Microstructure of nodular cast iron grade FCD 500

The graphite spheroids provide improvement in mechanical advantages compared to the graphite flakes in gray cast iron. Nodular cast iron is similar to gray cast iron in having a low melting point, good fluidity, castability, excellent machinability and wear resistance. However compared to gray cast iron, nodular cast iron has improved in strength, ductility toughness and hot workability.

Nodular cast iron as found wide acceptance and competes favourably with steel such that its use in engineering has increased in recent times while gray cast iron and malleable cast iron has fallen in popularity compared to other materials such as plastics that have found favor.

Nodular cast iron has a clear advantage over malleable cast iron for applications where low solidification shrinkage is needed or where the section is too thick to permit uniform solidification as required in white cast iron (Solidification as white cast iron throughout a section is essential to the production of malleable cast iron) [5].

2.2 Problem in weldability of cast iron

Under a welding thermal cycle, the cast iron base metal promptly close to the weld metal is locally heated to an extremely high temperature, this leads to two regions having quite high cooling rates, as presented in Figure 2.

2.2.1 *The fusion boundary*, the area adjacent to the weld metal, cementite tends to precipitate in this area called the white-cast-iron-zone [1].

Cementite, also called iron carbide, has a chemical compound of iron and carbon, with the formula Fe_3C . It is 6.67% carbon and 93.3% iron. It is hard and brittle [6].

2.2.2 *The heat affected zone (HAZ)*, the region beside the base metal, high-carbon martensite characterized by the hard and brittle nature contributes to form in this part known as the martensite zone [1].

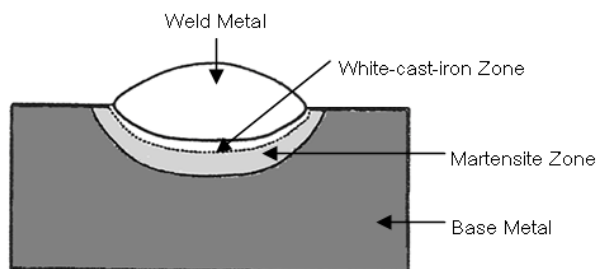


Figure 2: Microstructural of a typical cast iron weldment [1]

3 Experimental work

3.1 Material and Equipment

The welding material applied in this study was nodular cast iron grade FCD 500 whose dimensions were 300 x 150 x 38 mm. The samples were machined and prepared for welding with a single U-groove with 70° of groove angle. The depth of groove was 18 mm, as displayed in Figure 3.

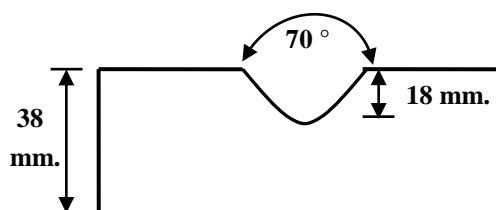


Figure 3: The preparation of groove in nodular cast iron grade FCD 500

3.2 Welding Procedure

The two specimens were surfaced; multi-pass bead on-plate welds were deposited on the flat position utilizing manual SMAW process. The first specimen used only ENiFe-CI electrode, as shown in Figure 4.

And the second specimen employed ENiFe-CI electrode for buttering the groove and E7016 electrode for subsequent layers, as displayed in Figure 5.

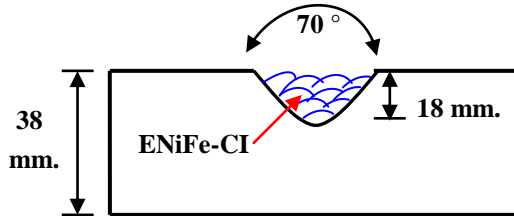


Figure 4: The first pattern of using filler metal in the groove of nodular cast iron grade FCD 500 when the SMAW ENiFe-CI filler metal is operated

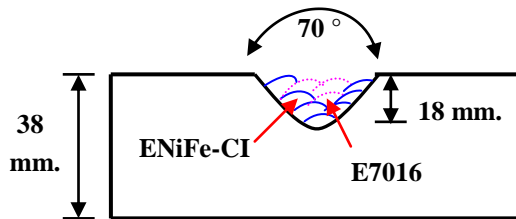


Figure 5: The second pattern of employing filler metal in the groove of nodular cast iron grade FCD 500 when the SMAW ENiFe-CI filler metal is operated

In addition, as required by the electrode manufacturers and welding technique, the welding sequence in each bead is required to be welded at the maximum length of 5 centimetre. The layout of each bead would be back-step welding. It is also required hot peening on each weld prior start the next 5 centimeter weld.

The level of preheat was 300°C for 2 hrs and the interpass temperature should be not greater than 350°C. After the welding was performed, the samples were immediately transferred to a furnace and held there for 2 hrs at 650°C and then furnace-cooled to room temperature. The welding parameters were presented in Table 1.

3.3 Testing methods

Each weld was examined by Liquid Penetrant Testing (PT) for locating discontinuities on the surface before evaluating metallographic and mechanical property. Cutting specimen for metallographic examination was achieved by avoiding excessive heating that might have led to local variation in the microstructure.

Standard preparation techniques were operated to reveal the microstructure using a nital 2% solution. Vickers microhardness test (1000 g load) was done on the polished and etched surface. Microhardness tests were performed on the longitudinal welds from the weld metal to the base metal.

Table 1: Welding parameters

	ENiFe-CI	E7016
Current, DC	60-90 A	90-130 A
Volt	22 – 25 V	20 – 28 V
Electrode Dia.	2.6 mm	3.2 mm
Travel speed	80 – 120 mm/min	120 – 150 mm/min
Preheat Temp.: 300°C		
Interpass Temp.: 350°C Max		
PWHT: 650°C for 2 hrs		

4 Results and discussion

4.1 Microhardness and microstructure of the welds of nodular cast iron grade FCD 500 using ENiFe-CI filler metal

Figure 6 and Figure 7 indicate the typical curve for Vickers microhardness vs distance of the welds of nodular cast iron grade FCD 500 applying ENiFe-CI and ENiFe-Ci plus E7016 electrode respectively. Following the curve from left to right, the hardness values correspond initially to the weld metal, and then the hardness value increases at the fusion boundary. The hardness values decrease at the heat affected zone and continued to the hardness values corresponding to the base metal.

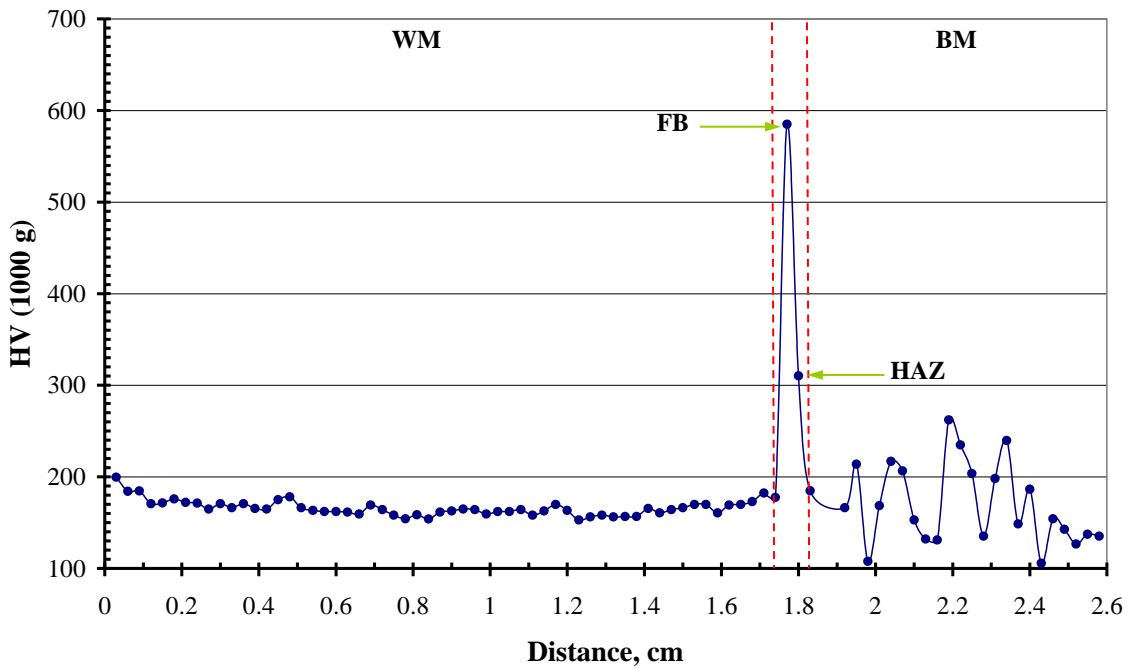


Figure 6: Microhardness distribution in the different zones of the welds of nodular cast iron grade FCD 500 when the SMAW ENiFe-CI filler metal is operated

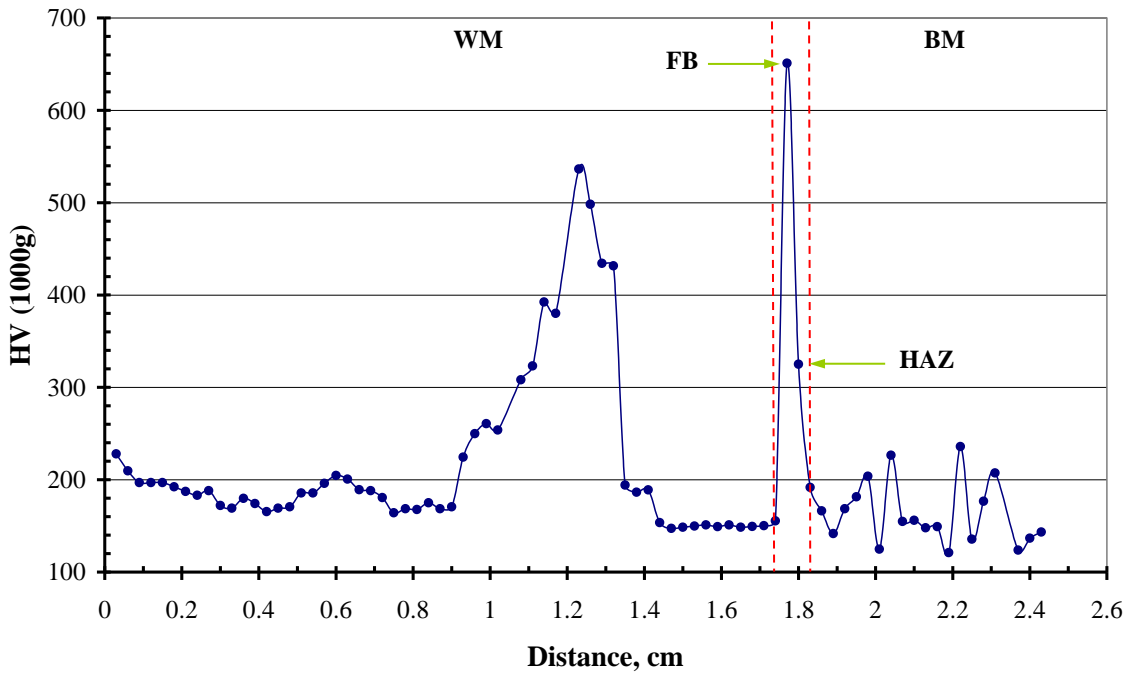


Figure 7: Microhardness distribution in the different regions of the welds of nodular cast iron grade FCD 500 when the SMAW ENiFe-CI and E7016 filler metal are utilized

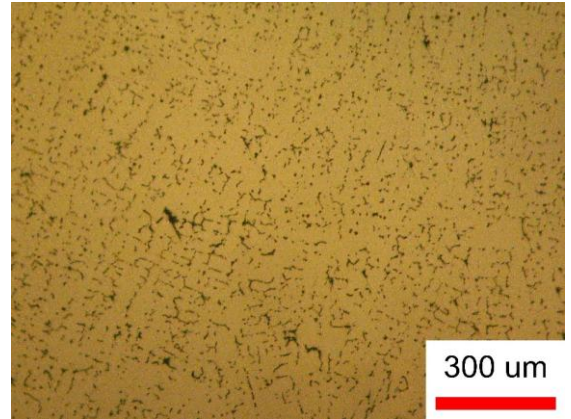
The average hardness value in the weld metal (Figure 6, from 0.03 to 1.74 cm) comprising ENiFe-CI electrode is about 170 HV. Austenite with ferrite at the sub-grain boundary is formed in this area, as displayed in Figure 8(a).

Next to the weld metal, the hardness values increase (Figure 6, from 1.74 to 1.83 cm) because the various phases are detected at the interface, as shown in Figure 8(b). The hardness value in the fusion boundary (Figure 6, at 1.77 cm) is 585 HV as accounted of appearing very hard and brittle ledeburitic carbides as a result of fast cooling condition [2, 7].

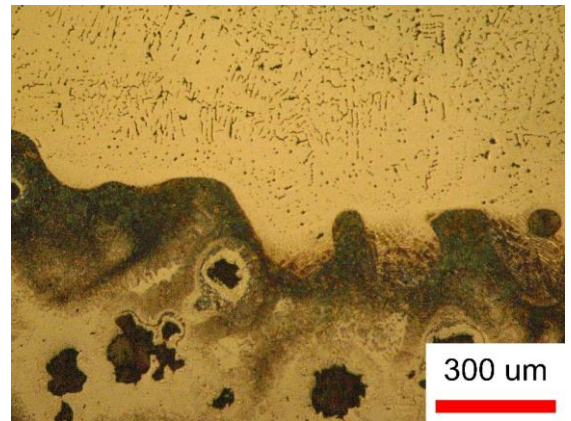
Moving into the base metal it is seen that, melting begins at cell boundaries and nodules matrix interfaces, the parent graphite nodules are surrounded by a thin ring “halo” of ledeburitic carbides. This morphology results from rapid cooling rates from the melt in which the graphite nodules were dissolved and fragmented [2]. In the heat affected zone, there is the formation of bainite from the solid state transformation of austenite [7]. The average hardness value in this area (Figure 6, from 1.77 to 1.83 cm) is 310 HV.

In the base metal, the average hardness area (Figure 6, from 1.83 to 2.58 cm) is around 165 HV since this region consists of graphite nodules surrounded by ferrite rings and the darker lamellar structure in the matrix known as pearlite. This typical structure is described as a bull’s eye pattern [2], as presented in Figure 8(c).

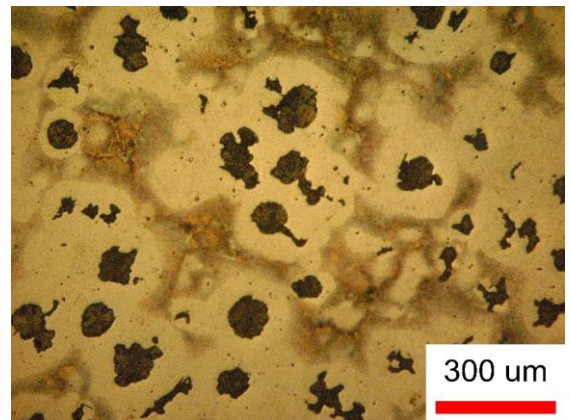
From Figure 6, The fluctuation of the hardness values in the base metal results from diverse structures. The average hardness of the spheroidal graphite - such as at 1.98 and 2.43 cm - is approximately 100 HV. The average hardness of pearlite, like at 2.19 and 2.34 cm, is roughly 230 HV. In addition to, the average hardness of the ferrite ring (such as at 1.98 and 2.43 cm) is about 175 HV.



8(a) Weld metal (ENiFe-CI filler metal)

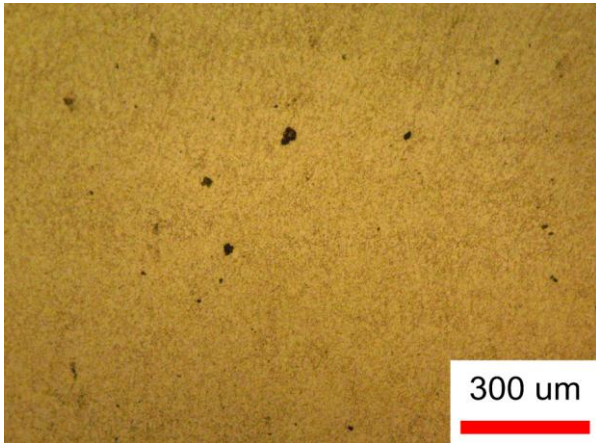


8(b) Interface

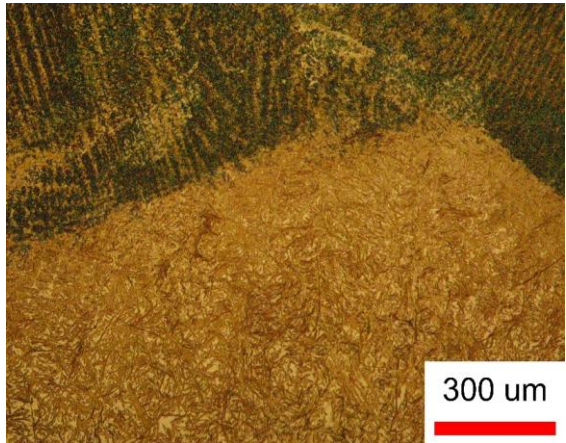


8(c) Base metal

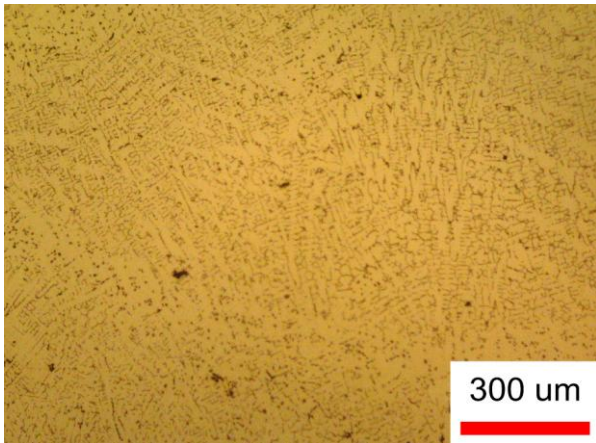
Figure 8: Microstructure in the different areas of the welds of nodular cast iron grade FCD 500 when the SMAW ENiFe-CI filler metal is employed



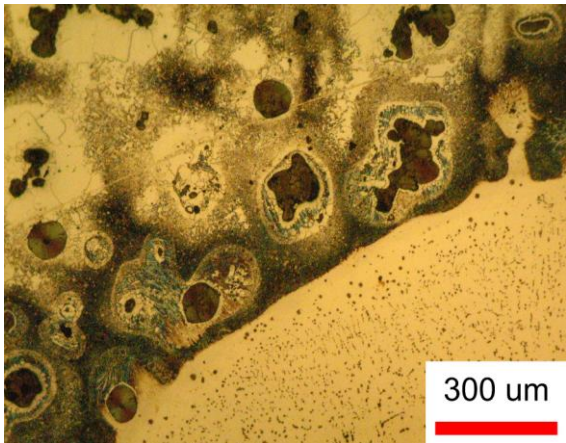
9(a) Weld Metal (E7016 filler metal)



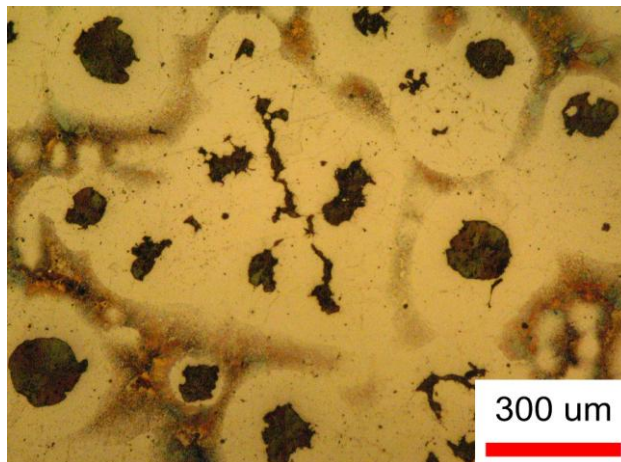
9(b) Weld Metal (Bottom of E7016 electrode)



9(c) Weld Metal (ENiFe-CI filler metal)



9(d) Interface



9(e) Base Metal

Figure 9: Microstructure in the different areas of the welds of nodular cast iron grade FCD 500 when the SMAW ENiFe-CI and E7016 filler metal are used

4.2 Microhardness and microstructure of the welds of nodular cast iron grade FCD 500 employing ENiFe-CI and E7016 filler metal

Figure 7 demonstrates the typical curve for Vickers microhardness vs distance of the welds of nodular cast iron grade FCD 500 utilizing ENiFe-CI and E7016 electrode. Following the curve from left to right, the hardness values correspond firstly to the weld metal as E7016 electrode, and then the hardness values heighten in the weld metal using E7016 electrode adjacent to ENiFe-CI electrode. The hardness values diminish in the weld metal utilizing ENiFe-CI filler metal, and then the hardness values increase at the fusion boundary. The hardness values lessen in the heat affected zone to the hardness values corresponding to the base metal.

The average hardness value in the weld metal (Figure 7, from 0.03 to 0.9 cm) containing E7016 filler metal is approximately 184 HV because of the formation of acicular ferrite, as shown in Figure 9(a). However, the average hardness at the bottom of the weld metal employing E7016 electrode that connects ENiFe-CI electrode (Figure 7, from 0.9 to 1.35 cm) is about 500 HV on account of the formation of martensite, as showed in Figure 9(b). Martensite formation in this region is associated not only the carbon diffusion from E7016 to ENiFe-CI electrode but also large amounts of alloying elements.

The average hardness value in the weld metal (Figure 7, from 1.35 to 1.74 cm) composed of ENiFe-CI electrode is about 152 HV. At the interface between the weld metal and the base metal, the hardness of the fusion boundary (Figure 7, at 1.77 cm) is 651 HV and that of the heat affected zone (Figure 7, at 1.8 cm) is 325 HV. The average hardness in the base metal (Figure 7, from 1.83 to 2.43 cm) is roughly 161 HV.

The structures in the weld metal comprising ENiFe-CI electrode, the interface and the base metal of this specimen, as presented in Figure 9(c), 9(d) and 9(e) respectively, are similar to those of the previous specimen.

5 Conclusions

5.1 At the weld metal, the use of ENiFe-CI and E7016 filler metal relatively produces the lower hardness value in the account of containing austenite with ferrite at the sub-grain boundary and acicular ferrite respectively. On the other hand, at the bottom of the weld metal employing E7016 electrode

creates the higher hardness because of comprising martensite that results from carbon diffusion and large amounts of alloying elements.

- 5.2 At the interface, the highest hardness value appears in the fusion boundary because of the formation of ledeburitic carbides and hardness value slightly lowers in the heat affected zone due to the formation of bainite.**
- 5.3 The hardness value in the base metal is relatively quite low as this region consists of pearlite and graphite nodules surrounded by ferrite rings.**

Acknowledgments

I extend my sincere thanks to Assoc. Prof. Dr. Bovornchok Poopat and Dr. Isaratat Phung-on who supported and advised this research as well as the EGAT Nong Chok which contributed to preparing the welding specimen in this research.

References

- [1] Shinko Yamamoto., 2008. *Arc welding of Specific Steels and Cast Irons*, Shinko Welding Service, Japan, 4-1 – 4-18.
- [2] E.M. El-Banna., 1999. *Materials Letters, Effect of preheat on welding of ductile cast iron*, 41: 20-26.
- [3] M. Pascual, J. Cembrero, F. Salas, M. Pascual Martinez, 2007. *Materials Letters, Analysis of the weldability of ductile iron*, 62: 1359-1362.
- [4] Manat Sathirajinda., 2000. *Cast Iron*, Chulalongkorn University Printing House, Thailand, 36.
- [5] Roy Beardmore, 2010. *Cast Iron*, http://www.roymech.co.uk/Useful Tables/Matter/Cast_iron.html, England accessed on Aug 17, 2010
- [6] William F. Smith., 1996. *Principles of Materials Science and Engineering*, The McGraw-Hill Companies, Inc, 317.
- [7] E.M. El-Banna, M.S. Nageda and M.M. Abo El-Saadat., 1999. *Materials Letters, Study of restoration by welding of pearlitic ductile cast iron*, 42: 311-320.